NeuroImage 57 (2011) 1015–1021

Contents lists available at ScienceDirect

NeuroImage

journal homepage: www.elsevier.com/locate/ynimg

Clinical fMRI: Evidence for a 7 T benefit over 3 T

R. Beisteiner [a,c,*], S. Robinson [b,c], M. Wurnig [a,c], M. Hilbert [a,c], K. Merksa [a,c], J. Rath [a,c], I. Höllinger [a,c], N. Klinger [a,c], Ch. Marosi [d], S. Trattnig [b,c], A. Geißler [a,c]

[a] Study Group Clinical fMRI, Department of Neurology, Medical University of Vienna, Austria
[b] Department of Radiology, Medical University of Vienna, Austria, Währinger Gürtel 18-20, 1090 Vienna, Austria
[c] MR Center of Excellence, Medical University of Vienna, Austria, Währinger Gürtel 18-20, 1090 Vienna, Austria
[d] Department of Medicine I, Medical University of Vienna, Austria, Währinger Gürtel 18-20, 1090 Vienna, Austria

ARTICLE INFO

Article history:
Received 23 February 2011
Revised 2 May 2011
Accepted 3 May 2011
Available online 17 May 2011

Keywords:
fMRI
Ultra high field
Patient
Motor
Sensitivity

ABSTRACT

Despite there being an increasing number of installations of ultra high field MR systems (>3 T) in clinical environments, no functional patient investigations have yet examined possible benefits for functional diagnostics. Here we performed presurgical localization of the primary motor hand area on 3 T and 7 T Siemens scanners with identical investigational procedures and comparable system specific sequence optimizations. Results from 17 patients showed significantly higher functional sensitivity of the 7 T system measured via percent signal change, mean t-values, number of suprathreshold voxels and contrast to noise ratio. On the other hand, 7 T data suffered from a significant increase of artifacts (ghosting, head motion). We conclude that ultra high field systems provide a clinically relevant increase of functional sensitivity for patient investigations.

Introduction

The number of ultra high field MR systems, mostly 7 T systems, installed in environments with clinical connections is steadily increasing. Based on a higher signal to noise ratio, expectations are that 7 T systems will improve clinical diagnostics. This also includes functional diagnostics, which relies on increased sensitivity to the BOLD (Blood Oxygenation Level Dependent) effect (Olman et al., 2010; van der Zwaag et al., 2009).

Despite this background, results from 7 T patient studies are yet scarce. A small number of initial patient investigations and feasibility studies have compared 7 T data with data from 3 T, 1.5 T or data from literature. They have indicated 7 T benefits for morphological diagnostics, including improved detection of multiple sclerosis plaques (Kollia et al., 2009; Metcalf et al., 2010), improved detection of pathologies in Alzheimer's disease (Nakada et al., 2008) and improved classification of brain lesions (Moenninghoff et al., 2010; Tallantyre et al., 2009). Benefits have also been described for angiographic detection of small vessel changes in hypertensive patients (Kang et al., 2009) and spectroscopic investigations of brain tumors (Avdievich et al., 2009). However, to date, no functional patient investigations have been performed at 7 T to examine possible benefits for functional diagnostics (e.g. presurgical localization of essential cortical areas using fMRI).

Clinical fMRI offers considerable potential to reduce invasive diagnostic procedures and is already routinely applied in specialized diagnostic centers (for a recent review see Prayer et al., 2010). A recent fMRI study of healthy subjects comparing functional results at 1.5, 3 and 7 T showed several 7 T benefits based on an increased $\Delta R2^*/R2^*$ ratio (van der Zwaag et al., 2009). However, there are also several drawbacks of high field systems which may counteract improved BOLD sensitivity, in particular in patients with pathological brains. The most important issues are increased susceptibility artifacts, reduced homogeneity of the transmitted radiofrequency field and potentially larger motion artifacts. Due to brain pathology and the patients' limited abilities to cooperate, these issues may result in increased image distortions, local artifacts and signal dropouts compared to healthy subjects. As a consequence, it is currently not clear whether advantages or disadvantages of ultra high field systems prevail for functional clinical diagnostics.

Given the fact that clinical 3 T high field systems are now widely available, this study investigated whether there are diagnostic benefits for a standardized fMRI investigation when progressing from 3 T to 7 T in a clinical setting. A frequently requested presurgical localization of the primary motor hand area was chosen as clinically relevant task. We concentrated on results achievable with identical

* Corresponding author at: Study Group Clinical fMRI, Department of Neurology, Medical University of Vienna, Währinger Gürtel 18-20, 1090 Vienna, Austria. Fax: +43 1 40400 3459.
E-mail addresses: roland.beisteiner@meduniwien.ac.at (R. Beisteiner), simon.robinson@meduniwien.ac.at (S. Robinson), mwurnig@gmail.com (M. Wurnig), hilbert.fmri@gmail.com (M. Hilbert), merksa.fmri@gmail.com (K. Merksa), jakob.rath@meduniwien.ac.at (J. Rath), ilse.hoellinger@gmail.com (I. Höllinger), nicolaus.klinger@gmail.com (N. Klinger), christine.marosi@meduniwien.ac.at (C. Marosi), siegfried.trattnig@meduniwien.ac.at (S. Trattnig), alexander.geissler@meduniwien.ac.at (A. Geißler).

1053-8119
doi:10.1016/j.neuroimage.2011.05.010

investigational procedures and comparable system-specific sequence optimizations performed according to the current state of the art. Important clinical image parameters such as matrix size and field of view were kept constant, as was the analysis approach. Evaluation concentrated on key parameters for assessing functional sensitivity, including percentage signal change, contrast to noise ratio and statistical parameters within functional regions of interest (ROIs). Our hypothesis was that a clinically relevant benefit, evidenced through functional sensitivity, would be present for fMRI studies in brains affected by pathology at 7 T.

Materials and methods

Patients

Seventeen patients (6 females, mean age 40.5 years old and 11 males, mean age 25.3 years old; age range 9–70 years of age), consecutively referred for presurgical diagnostics, participated in the study (see Table 1 for demographic and clinical details). For all patients, a functional localization of the motor hand area for the clinically affected hand had been requested by physicians, for a number of reasons. No exclusion criterions were applied. At the time of measurement, all patients were of good general constitution, could move the relevant hand against resistance and could perform the motor task well. The study was approved by the ethics committee of the Medical University of Vienna. All patients gave written informed consent.

Task

The functional paradigm was a simple motor task: repetitive opening and closing of the affected hand with eyes open. The healthy hand was investigated in peripheral nerve patient P8 due to exceptional paresis (see Table 1). One run consisted of four rest (A) and three movement phases (B) of 20 s each presented in a blocked ABABABA design. Depending on the patient's tolerance, between four and eight runs were accomplished. Instructions – when to begin and when to stop the action – were communicated to the patients via headphones. Patients were requested to perform the task at a rate of 1 Hz (for each cycle of opening and closing the hand) and were assisted in achieving this via a visually presented indicator; a circle, which was cyan for 0.5 s, then red for 0.5 s. The visual input during rest phases was identical.

Table 1
Demographic and clinical details of the patients studied.

Patient	Sex	Age	Side of pathology	Pathological diagnosis at the time of fMRI
P1	f	34	Right	Frontal tumor, unknown origin
P2	m	28	Right	Frontal tumor, unknown origin
P3	m	16	Right	Parietooccipital malformations (Sturge Weber)
P4	m	70	Left	Central recurring glioblastoma
P5	m	21	Right	Temporal astrocytoma (II°)
P6	m	38	Left	Frontal low grade glioma
P7	f	32	Left	Temporal glioblastoma
P8	f	31	Right	End to side coaptation right phrenic nerve to right musculocutaneous nerve after complete brachial plexus lesion right. fMRI data from the healthy left hand.
P9	m	11	Right	Fronto-central focal cortical dysplasia
P10	m	14	Right	Cryptogenic temporal lobe epilepsy
P11	m	9	Left	Central focal cortical dysplasia
P12	f	38	Left	Opercular oligoastrocytoma (II°)
P13	f	55	Left	Left pre-central tumor, unknown origin
P14	m	21	Right	Central low grade glioma
P15	m	21	Left	Post-central polycystic astrocytoma
P16	m	29	Right	Postcentral tumor, unknown origin
P17	F	53	Left	Parietal tumor, unknown origin

Image acquisition

Patients were examined with both a 3 T Siemens MAGNETOM TIM TRIO scanner and a 7 T Siemens MAGNETOM scanner (Siemens, Erlangen, Germany). Measurements at the two field strengths were typically carried out within 10 days. However, for clinical reasons, for 2 patients this interval had to be increased (to 37 days for P11, to 62 days for P12). To minimize head motion artifacts, individually constructed plaster cast helmets (Edward et al., 2000) were used on both systems. A 32 channel Siemens head coil (Siemens, Erlangen, Germany) was used for 3 T measurements. For 7 T measurements, a 24 channel head coil was applied for P1–P15, while – due to a system upgrade involving a coil exchange – P16 and P17 were measured with a 32 channel head coil (both manufactured by Nova Medical, Wilmington, Massachusetts, USA). On both systems, functional MRI data were acquired with a 2D single-shot gradient echo (GE) EPI sequence, with slices aligned parallel to the AC-PC plane and whole brain coverage. Simple system-specific sequence optimizations were performed according to requirements for whole brain coverage and recommendations in the literature.

Common sequence parameters

FOV 230 mm, matrix size $128\times128\times34$, 56 repetitions, slice thickness 3 mm, TR: 2500 ms, parallel imaging with GRAPPA-iPAT factor 2, fat suppression by a chemical shift selective saturation pulse prior to every slice, 10 s of dummy scans.

Differing sequence parameters

3 T: TE 28 ms, bandwidth 2220 Hz, flip angle 90°, full Fourier encoding, no gap between slices. Vendor provided fat saturation module with a preset flip angle of 110°.

7 T: TE 22 ms, bandwidth 1445 Hz (P1 1220 Hz, P4 1395 Hz to reduce ghosting), flip angle 80°, 6/8 partial Fourier factor (omitting the first 25% of k-space phase-encoding lines), 10% gap between slices. The effective echo time at 7 T was optimized via assessment of T2* for this resolution. Flip angles of the vendor-provided fat saturation module were reduced to 90° due to specific absorption rate (SAR) limitations.

At each field strength, high-resolution sagittal T1-weighted MR images were acquired using a 3D MPRAGE sequence for visualizing anatomical details. However, these images did not enter data analysis in the current study.

fMRI data analysis

Functional data were pre-processed and statistical analysis was performed using SPM8 (Wellcome Department of Imaging Neuroscience, London, UK; http://www.fil.ucl.ac.uk/spm). To reduce residual small-scale motion, all runs were registered to the first scan using default settings except for the factors “Quality: 0.95” and “Separation: 2”, both chosen to improve correction quality. No slice timing correction or spatial normalization was carried out. Functional images were smoothed with a $4\times4\times6$ mm full width at half maximum (FWHM) Gaussian kernel. First level statistical analysis was performed with a mixed effects analysis (default settings, no additional temporal filtering or averaging) with inclusion of motion parameters in the design matrix as nuisance variables. BOLD responses were modeled by a fixed response boxcar function convolved with the canonical hemodynamic response. Activation was established for each patient via voxel-wise t-tests to generate individual SPM t-maps. The same number of 3 T and 7 T runs were analyzed for each patient. All superfluous runs were excluded (by acquisition order, to avoid bias).

Definition of functional ROIs

First, individual neuroanatomical ROIs comprising the inverted omega structure around the central sulcus (the primary motor hand area) were manually defined by a neurologist (Figs. 1 and 2). The ROI definitions were carried out separately for each field strength. All activated voxels ($p<=0.05$, family-wise error (FWE) — corrected, (Nichols and Hayasaka, 2003)) within the predefined ROI formed the resulting functional ROI. The validity of the functional ROIs was verified by visually inspecting individual SPM t-maps superposed on an individual EPI image (mean image after realignment). Given that the size of regions identified as being active may increase with the field strength, this procedure assured inclusion of all relevant primary motor activations and reduced the influence of non-primary cortex activity on final results.

Data quantification

To assess effects related to the two field strengths, we analyzed only significant voxels in the functional ROIs and compared six measures relevant to functional activation: (1) voxel count (number of supra-threshold voxels), (2) mean t-value, (3) peak t-value, (4) percentage signal change, (5) contrast to noise ratio (CNR) (Geissler et al., 2007) and (6) peak CNR. To evaluate relevant sources of artifacts, a metric for head motion and a ghost to signal ratio were also calculated.

Quantification of functional activation

Measures (1) Voxel count, (2) Mean t-value and (3) Peak t-value. For each patient, all voxels included in the functional ROIs (fROIs) were separately analyzed for the 3 T and 7 T experiments. The voxel count (the number of voxels in the fROI), the mean t-value of all fROI voxels and the highest t-value of all fROI voxels were determined.

Measure (4) Percentage signal change. Percentage signal change, $\Delta S/S_{OFF}$, was calculated according to the definition of van der Zwaag et al. (2009, c.f. section "Analysis"). In brief $\Delta S = (S_{ON}\text{-}S_{OFF})$, where S_{ON} is the mean absolute signal of all time points within "ON" phases and S_{OFF} is the mean of all time points within "OFF" phases (arithmethic mean, voxel-wise calculation). For the definition of ON and OFF phases the underlying block design of the paradigm was shifted by five seconds to accord with the delayed BOLD response. This calculation was performed for all voxels within the fROI separately for every run of each patient followed by arithmetic averaging to achieve one representative figure per patient and field strength.

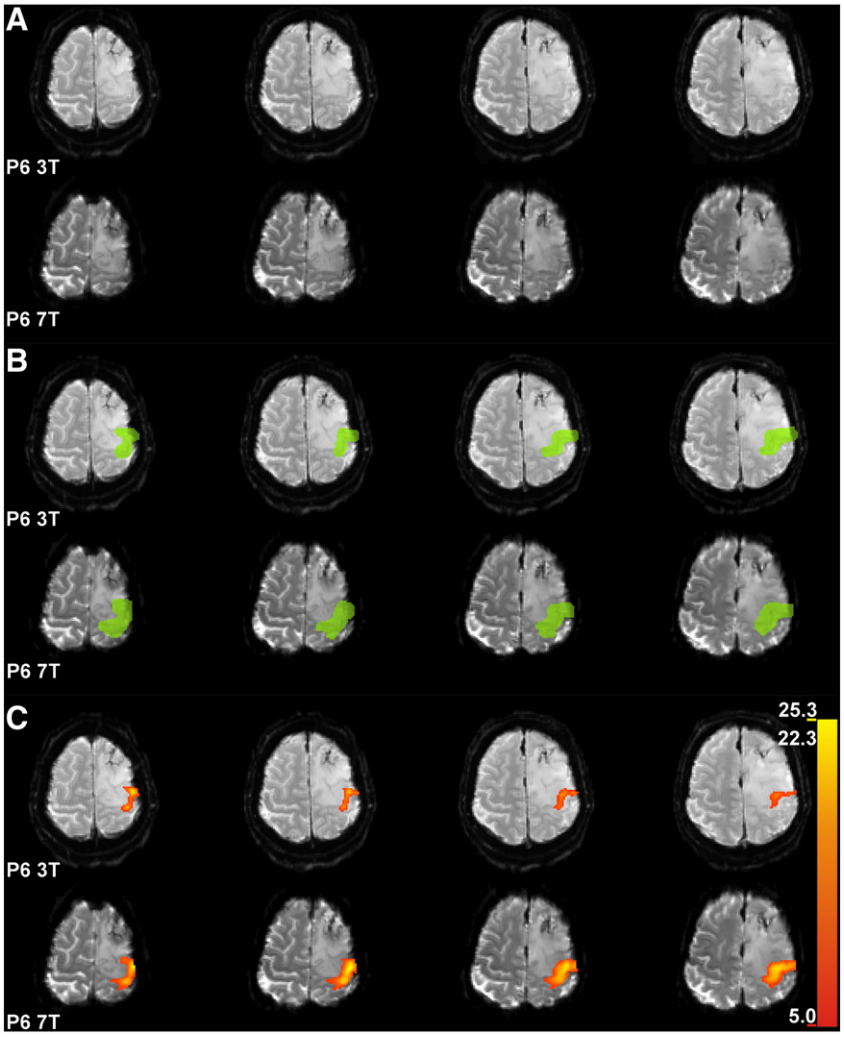

Fig. 1. Patient P6. A: Functional EPI slices covering central parts of the primary motor hand area at 3 T and 7 T. B: Same as A with neuroanatomical ROIs depicting the primary motor hand area (light green). C: Same as B with depiction of all suprathreshold voxels ($p<=0.05$, FWE — corrected) within the neuroanatomical ROIs. Only these voxels entered statistical analysis and formed the functional ROI. Color bar indicates t-values of active voxels (3 T maximum = 22.3, 7 T maximum = 25.3).

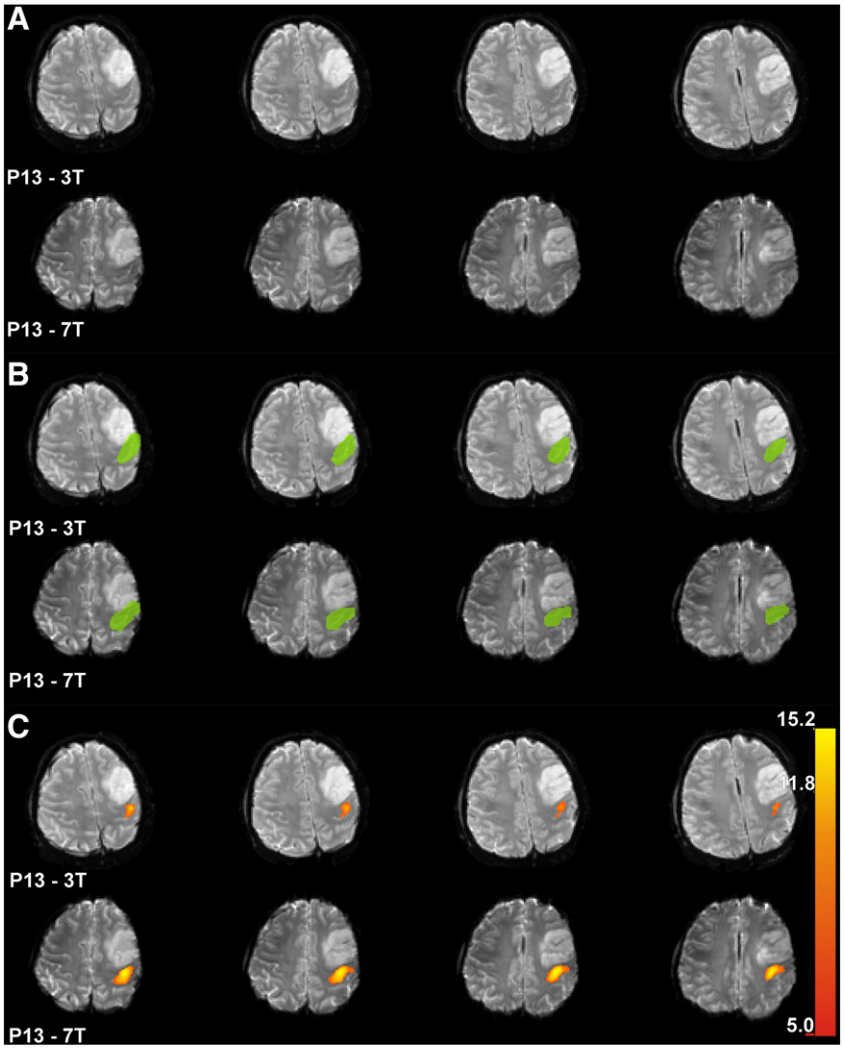

Fig. 2. Patient P13. Same es Fig. 1. 3 T t-value maximum = 11.8, 7 T t-value maximum = 15.2).

Measures (5) Contrast to noise ratio (CNR) and (6) Peak contrast to noise ratio. CNR was calculated from $\Delta S_{CNR}/\sigma_{t\text{-}noise}$, as defined in Geissler et al. (2007), paragraph "*CNR Calculation Using Savitzky-Golay (SG) Filters (CNR_SG)*". Essentially, the contrast ΔS_{CNR} is the averaged voxel-wise signal change in the temporally smoothed original signal: (mean value of all time points within the "ON" phase) – (mean value of all time points within the "OFF" phase). ON/OFF definitions were the same as for the percentage signal change analysis (measure 4, see above). Smoothing was performed using a Savitzky–Golay filter with a polynomial order of 2 and length 5. $\sigma_{t\text{-}noise}$ is the non-task-related variability over time — in this case the standard deviation of the difference between the original and smoothed signals. Again, this calculation was done for all voxels within the functional ROI and every run of each patient, followed by arithmetic averaging to achieve one representative number per patient and field strength. The patient's peak CNR was determined by analyzing the mean CNR values of all ROI voxels separately for the 3 T and 7 T experiments to detect the voxels with the largest 3 T / 7 T CNR.

Calculation of motion indicator for head motion quantification

Head motion was quantified at both field strengths using the parameters resulting from the motion correction procedure of SPM8. It was hypothesized that head motion may differ between MR systems due to the different dimensions of the magnet (3 T/7 T = 2.13 m/4 m length), head coils and head fixation helmets (Edward et al., 2000). To evaluate head motion, a global parameter was calculated separately for translation and rotation. Translation: integrating x-, y-, and z-axis values, the Euclidian distance (in mm) between successive volumes was determined for every run. The median of these between-volume distances was taken used as a single-parameter metric for motion. Rotation: for each angle (pitch, roll, yaw) between-volume rotations were assessed and the median between-volume rotation (in rad) was determined over all volumes of all runs per patient and axis.

Calculation of ghost to signal ratio for quantification of ghosting artifacts

Parallel imaging (PI) allows phase-encoding steps to be omitted, enabling resolution to be increased (while achieving the same effective echo time) and distortion to be decreased. In this study, generalized auto-calibrating parallel acquisition (GRAPPA) factor 2 was used at both field strengths (Griswold et al., 2002). With acceleration, image quality is reduced by patient motion, which affects the applicability of reference lines and leads to ghost-like artifacts (Skare et al., 2007). To determine the magnitude of these artifacts we defined a ghost to signal ratio similar to that defined in the EU COMAC-BME II project (Lerski and de Certaines, 1993). Two types of ROIs were defined (Fig. 3): a central reference ROI — in a homogenous region of white matter within the brain and one anterior and one posterior ghosting ROI — comprising ghosting artifacts occurring in the phase-encode direction. ROI selection was performed within three slices adjacent to the central slice of the EPI dataset. For

every patient, the ghost to signal ratio was calculated as the ratio between the mean absolute signal within the ghosting ROIs to the mean signal in the central reference ROI.

Statistical evaluation of 3 T–7 T differences

After testing for normal distribution, paired t-tests comparing 3 T and 7 T values were calculated over all patients for voxel count, mean t-value, peak t-value, percentage signal change, CNR, peak CNR, motion indicator and ghost to signal ratio.

Results

The primary metrics described in "Data quantification" are summarized in Table 2 for 3 T and 7 T measurements. All measures of functional activation showed a statistically significant benefit for the 7 T system, except for peak t-value, which showed no significant difference between 3 T and 7 T data. None of the measures indicated advantage for the 3 T system. Figs. 1 and 2 show typical activation changes from 3 T to 7 T. Fig. 4 illustrates the mean signal and CNR increase with the 7 T system.

While functional signal changes were greater, 7 T measurements suffered from a significant increase in artifacts: translational head motions were significantly larger (c.f. Fig. 5, rotation n.s.) and ghosting was substantially increased (see Fig. 6).

As part of a hardware upgrade the 24-channel coil which was used for the study of patients P1-15 was replaced by a 32-channel coil, which was used for measurement of P16 and P17. The main results – significant improvement in all performance metrics other than peak t-value – hold if P16 and P17 are excluded from the analysis.

Table 2
Summary of results.

Measure	3 T Value (SD)	7 T Value (SD)	P-value
Voxel count	666 (292)	896 (385)	0.0007
Mean t-value	10.7 (2.4)	11.6 (2.1)	0.04
Peak t-value	24.7 (8.0)	25.6 (6.6)	n.s.
Percentage signal change (%, mean of fROI)	1.8 (0.5)	2.3 (0.7)	0.004
Contrast to noise ratio (CNR)	3.3 (0.7)	4.3 (0.8)	0.00000002
Peak CNR	9.7 (3.2)	13.0 (3.3)	0.0000001
Motion indicator — Translation (mm)	0.04 (0.03)	0.09 (0.06)	0.005
Motion indicator — Rotation (rad)			
Pitch	1.9E-5 (4.5E-5)	2.0E-5 (1.1E-4)	n.s.
Roll	5.4E-6 (5.1E-5)	1.0E-5 (3.7E-5)	n.s.
Yaw	1.5E-6 (8.2E-5)	2.8E-5 (1.8E-4)	n.s.
Ghost to signal ratio	0.05 (0.02)	0.13 (0.07)	0.00007

Discussion

This study provides first data on the possible benefit of ultra high field systems for clinical fMRI. It is well known that imaging problems such as geometric distortions, signal dropouts and B1 inhomogeneity increase at very high field. The deleterious effects on functional images of pathological brains are not known. Correspondingly, it is not clear whether the potential benefits of 7 T systems may be realized in practice in clinical fMRI.

Previous ultra high field studies performed with healthy subjects typically used limited field of views (FOV) and, other than Gizewski et al. (2007) no functional whole brain coverage e.g. (Duong et al., 2003; Olman et al., 2010; van der Zwaag et al., 2009; Yacoub et al., 2001). This was due to technical limitations in some first-generation scanners and also to SAR limitations. However, the typical demand for a clinical application is whole brain coverage, since shifts of essential cortical areas due to pathology and functional reorganization are not predictable prior to the functional investigation. Another important problem with pathological brains concerns errors introduced by registration/normalization procedures or atlas-based region of interest definitions (Beisteiner et al., 2010; Gartus et al., 2007). To account for these issues, we performed whole brain coverage with a multichannel coil and a sub-maximal but clinically typical spatial resolution and data analysis on non-transformed individual functional images. The application of multichannel coils in this study enabled parallel imaging to be applied, which effectively reduced image distortions. Our motor task was standardized by visual triggering and represented a typical clinical paradigm which assured similar performance in both MR systems.

We performed a standard SPM8 data analysis with all individual data sets (FWE<0.05, motion parameters included as covariates of no interest, independent analysis of 3 T and 7 T data) and defined functional ROIs (fROIs) for primary motor hand activation. With the given task and an adequate amount of functional data, fROI definitions are possible with high reliability in pathological brains (Roessler et al., 2005). Our data analysis approach reduces the influence of non-primary cortex activity on the final results and minimizes effects related to postprocessing data transformations. To allow a comprehensive interpretation of 3 T–7 T differences and common grounds with previous studies (e.g. van der Zwaag et al., 2009), several measures were extracted from the functional ROIs: voxel count, mean t-value, peak t-value, percentage signal change, contrast to noise ratio (CNR) and peak CNR. The CNR analysis allows investigation of the data with minimal model assumptions, since it is not dependent on the shape of the hemodynamic response function but only on the mean signal increase during the "ON" phase (Geissler et al., 2007). As with

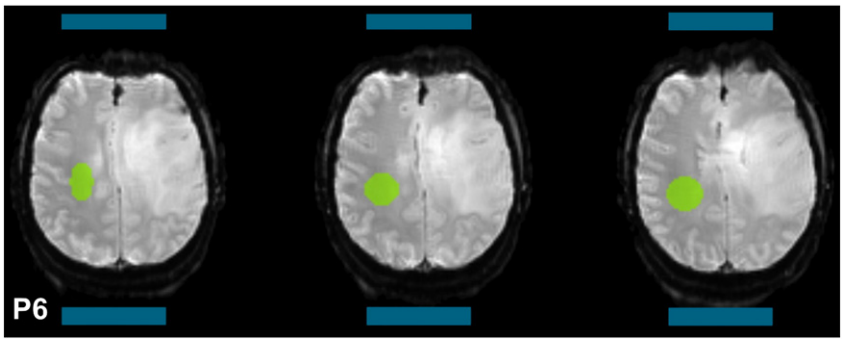

Fig. 3. Position of ROIs for quantification of ghosting artifacts (P6, 3 T data). Blue: ROIs for detection of ghosting signals, Green: central reference ROI. The relation between the mean absolute signals within the ghosting ROIs to the reference ROIs was calculated.

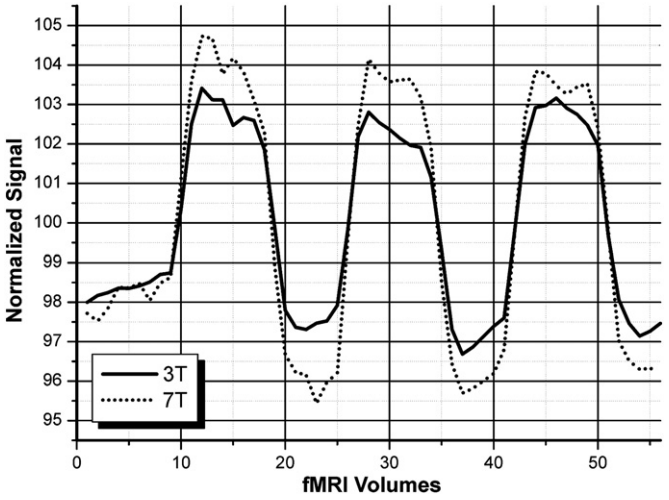

Fig. 4. Signal time course differences averaged over all peak CNR voxels of all patients.

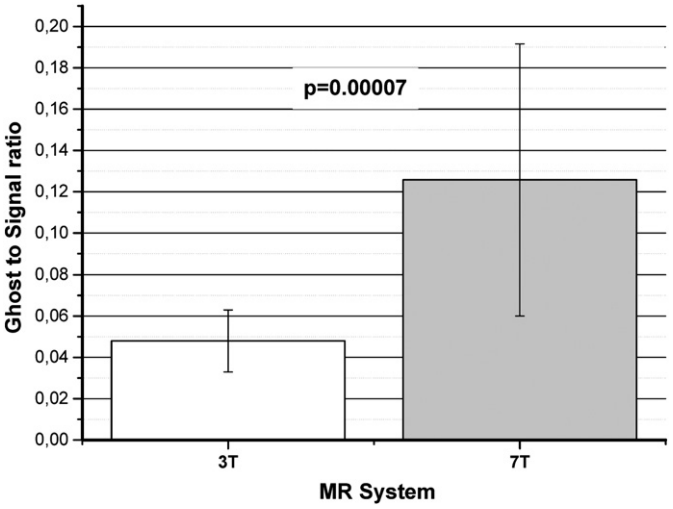

Fig. 6. Quantification of ghosting signals. The ghost to signal ratio is significantly larger with the 7 T system. Data show mean and standard deviation of the patient specific ghost to signal ratios.

every fMRI study such measures depend on the statistical thresholds used. However, for every clinical report a threshold needs to be defined (see discussion in (Beisteiner et al., 2010)). Here we used identical statistical models for 3 T and 7 T data and a well established threshold (FWE $p<0.05$) often used for clinical reports. Therefore, we consider it justified to regard these results as being relevant for patient investigations. Since our focus was on evaluating final fMRI results typically used for generating clinical reports – and corresponding to most previous studies investigating BOLD signal changes as a function of field strength – we did not directly measure the effect of changes of relaxation rates on activation. However, we evaluated the possible influence of typical sources of artifacts by quantifying the amount of ghosting and head motion.

The results demonstrate a significant 7 T benefit for all functional measures apart from peak t-value. The latter finding might be related to the increased artifact contamination of the 7 T data which might have more impact when comparing individual voxels instead of clusters. Patients showed significantly more head motion in the 7 T system, most probably due to the inferior head fixation (due to space restrictions in the 7 T head coil) and inferior comfort compared to the clinical 3 T system (space, noise, light…). In addition, ghosting artifacts were significantly larger in our 7 T images. Given the 3 T/7 T

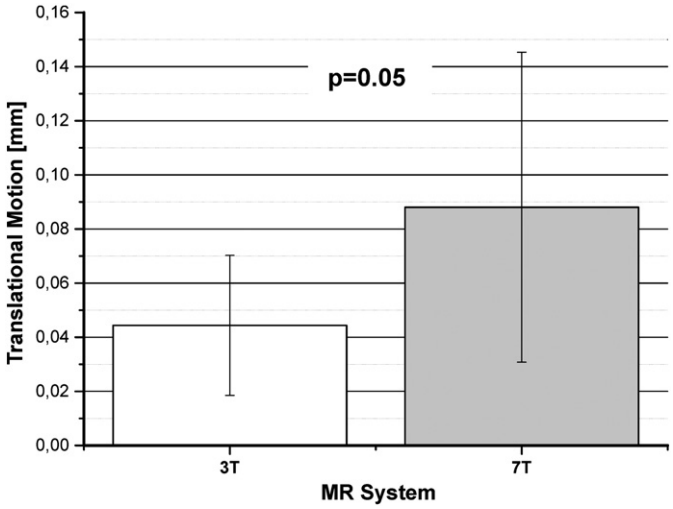

Fig. 5. Quantification of head motion. Translational head movements between two consecutively recorded brain volumes are larger with the 7 T system. Data show mean and standard deviation of the patient specific motion indicators.

experimental standardizations and application of standard thresholds, increase of activation sensitivity and activation volume should be a direct consequence of better SNR/CNR at 7 T. This corresponds to previous literature e.g. (Logothetis et al., 2001) which indicates that the fMRI signals „underestimate a great deal of actual neural activity". Further, investigations concerned with sensitivity for tissue/draining veins indicate that there should also be a benefit for reduced sensitivity to larger and draining veins (relative to sensitivity for tissue signals) at 7 T (Duong et al., 2003; Gati et al., 1997; Ogawa et al., 1998; Yacoub et al., 2001). The patients investigated in this study represent a typical clinical population. Inclusion was based solely on requests for motor localizations that were not influenced by the authors. It is also notable that we limited our procedures to system-specific setup and simple sequence optimizations performed according to the literature (e.g. Speck et al., 2008) — an approach feasible in every clinical context. The measurements were clinically standardized (including identical spatial resolution and whole brain coverage) and both MR systems were from the same manufacturer and current technical state of the art (including identical gradients and commercially available multi-channel head coils with a similar basic design and number of channels). Our results therefore represent realistic clinical outcome conditions and indicate that a functional 7 T benefit is not limited to special application conditions such as preselected patients or atypical coils and fMRI sequences. Interestingly, our findings are quite similar to previously reported results in healthy subjects, where significant 7 T benefits were established for voxel count, mean t-value and percentage signal change (van der Zwaag et al., 2009, CNR analysis was not performed). Therefore the benefit for patients accords well with that established with normal subjects. Of course, our results cannot be extrapolated to other fMRI paradigms or areas of the brain more prone to artifacts (inferior frontal cortex, basal temporal cortex). Such investigations have yet to be undertaken.

It is evident that comparisons of fMRI results from different MR systems may be influenced by numerous factors including hardware specifications, hardware quality, coils, software specifications, MR sequence details and differing patient states due to differing system environments. For example, it has been shown that high-field benefits are greatest at high resolution, a regime in which physiological noise is smallest relative to the thermal noise (Triantafyllou et al., 2005). However, Triantafyllou et al. also show that the tSNR gain for 7 T over 3 T reaches a maximum for voxel sizes of about $2\times2\times3$ (at ratio of approximately 1.32). Further reductions in voxel size bring no additional increase in the ratio of tSNR measured at 7 T compared to

3 T. The resolution used here was close to that at which Triantafyllou et al. observed the greatest increase in time-series SNR at 7 T over 3 T, so at most only a modest benefit is to be expected for comparison studies carried out at higher spatial resolution.

The MR environment may influence the general arousal state, which may also have consequences for the fMRI results (Nagai et al., 2004). Although we were able to establish comparability of final results for a clinical context (for instance, by applying a spatial standard resolution and matched measurement times), it is evident that the full potential of 7 T systems has not yet been exhausted with our setup. In fact, many factors differing between the 3 T and 7 T measurement in this study benefit the 3 T measurements. In the 3 T study we used a 32-channel coil (whereas most 7 T measurements were made with a 24–channel coil), full Fourier encoding, better head fixation and a more comfortable environment. The latter two factors led to markedly less head motion. The single (and modest) advantage in the 7 T study was the 10% gap allocation. Quite obviously, it is not possible to establish "identical" hardware setups and exact replications of sequence parameters or carry out a functional study with systematic variation of all relevant parameters. Additional investigations are required to clarify which parameter optimizations are most promising for a further increase of 7 T functional signal benefits in a clinical context.

Despite these qualifications, we conclude that 7 T systems enable a clinically relevant increase in functional sensitivity for patient investigations.

Acknowledgment

This study was supported by the Austrian Science Fund (P18057-B13) and the Vienna Spots of Excellence Programme „VIACLIC". We are grateful to FPS Fischmeister for critical input into the manuscript.

References

Avdievich, N.I., Pan, J.W., Baehring, J.M., Spencer, D.D., Hetherington, H.P., 2009. Short echo spectroscopic imaging of the human brain at 7 T using transceiver arrays. Magn. Reson. Med. 62, 17–25.

Beisteiner, R., Klinger, N., Hollinger, I., Rath, J., Gruber, S., Steinkellner, T., Foki, T., Geissler, A., 2010. How much are clinical fMRI reports influenced by standard postprocessing methods? An investigation of normalization and region of interest effects in the medial temporal lobe. Hum. Brain Mapp. 31, 1951–1966.

Duong, T.Q., Yacoub, E., Adriany, G., Hu, X., Ugurbil, K., Kim, S.G., 2003. Microvascular BOLD contribution at 4 and 7 T in the human brain: gradient-echo and spin-echo fMRI with suppression of blood effects. Magn. Reson. Med. 49, 1019–1027.

Edward, V., Windischberger, C., Cunnington, R., Erdler, M., Lanzenberger, R., Mayer, D., Endl, W., Beisteiner, R., 2000. Quantification of fMRI artifact reduction by a novel plaster cast head holder. Hum. Brain Mapp. 11, 207–213.

Gartus, A., Geissler, A., Foki, T., Tahamtan, A.R., Pahs, G., Barth, M., Pinker, K., Trattnig, S., Beisteiner, R., 2007. Comparison of fMRI coregistration results between human experts and software solutions in patients and healthy subjects. Eur. Radiol. 17, 1634–1643.

Gati, J.S., Menon, R.S., Ugurbil, K., Rutt, B.K., 1997. Experimental determination of the BOLD field strength dependence in vessels and tissue. Magn. Reson. Med. 38, 296–302.

Geissler, A., Gartus, A., Foki, T., Tahamtan, A.R., Beisteiner, R., Barth, M., 2007. Contrast-to-noise ratio (CNR) as a quality parameter in fMRI. J. Magn. Reson. Imaging 25, 1263–1270.

Gizewski, E.R., de Greiff, A., Maderwald, S., Timmann, D., Forsting, M., Ladd, M.E., 2007. fMRI at 7 T: whole-brain coverage and signal advantages even infratentorially? Neuroimage 37, 761–768.

Griswold, M.A., Jakob, P.M., Heidemann, R.M., Nittka, M., Jellus, V., Wang, J., Kiefer, B., Haase, A., 2002. Generalized autocalibrating partially parallel acquisitions (GRAPPA). Magn. Reson. Med. 47, 1202–1210.

Kang, C.K., Park, C.A., Lee, H., Kim, S.H., Park, C.W., Kim, Y.B., Cho, Z.H., 2009. Hypertension correlates with lenticulostriate arteries visualized by 7 T magnetic resonance angiography. Hypertension 54, 1050–1056.

Kollia, K., Maderwald, S., Putzki, N., Schlamann, M., Theysohn, J.M., Kraff, O., Ladd, M.E., Forsting, M., Wanke, I., 2009. First clinical study on ultra-high-field MR imaging in patients with multiple sclerosis: comparison of 1.5 T and 7 T. AJNR Am. J. Neuroradiol. 30, 699–702.

Lerski, R.A., de Certaines, J.D., 1993. Performance assessment and quality control in MRI by Eurospin test objects and protocols. Magn. Reson. Imaging 11, 817–833.

Logothetis, N.K., Pauls, J., Augath, M., Trinath, T., Oeltermann, A., 2001. Neurophysiological investigation of the basis of the fMRI signal. Nature 412, 150–157.

Metcalf, M., Xu, D., Okuda, D.T., Carvajal, L., Srinivasan, R., Kelley, D.A., Mukherjee, P., Nelson, S.J., Vigneron, D.B., Pelletier, D., 2010. High-resolution phased-array MRI of the human brain at 7 tesla: initial experience in multiple sclerosis patients. J. Neuroimaging 20, 141–147.

Moenninghoff, C., Kraff, O., Schlamann, M., Ladd, M.E., Katsarava, Z., Gizewski, E.R., 2010. Assessing a dysplastic cerebellar gangliocytoma (Lhermitte-Duclos disease) with 7 T MR imaging. Korean J. Radiol. 11, 244–248.

Nagai, Y., Critchley, H.D., Featherstone, E., Fenwick, P.B., Trimble, M.R., Dolan, R.J., 2004. Brain activity relating to the contingent negative variation: an fMRI investigation. Neuroimage 21, 1232–1241.

Nakada, T., Matsuzawa, H., Igarashi, H., Fujii, Y., Kwee, I.L., 2008. In vivo visualization of senile-plaque-like pathology in Alzheimer's disease patients by MR microscopy on a 7 T system. J. Neuroimaging 18, 125–129.

Nichols, T., Hayasaka, S., 2003. Controlling the familywise error rate in functional neuroimaging: a comparative review. Stat. Methods Med. Res. 12, 419–446.

Ogawa, S., Menon, R.S., Kim, S.G., Ugurbil, K., 1998. On the characteristics of functional magnetic resonance imaging of the brain. Annu. Rev. Biophys. Biomol. Struct. 27, 447–474.

Olman, C.A., Van de Moortele, P.F., Schumacher, J.F., Guy, J.R., Ugurbil, K., Yacoub, E., 2010. Retinotopic mapping with spin echo BOLD at 7 T. Magn. Reson. Imaging 28, 1258–1269.

Prayer, D., Foki, T., Beisteiner, R., Stippich, C., Woermann, F.G., Labudda, K., Furtner, J., Sachs, G., Kasprian, G., Seidel, S., Windischberger, C., Fischmeister, F.P.S., Schöpf, V., Sladky, R., Moser, E., 2010. Funktionelle MRT im klinischen Einsatz. Radiologe 50 (2), 103–151 Feb.

Roessler, K., Donat, M., Lanzenberger, R., Novak, K., Geissler, A., Gartus, A., Tahamtan, A.R., Milakara, D., Czech, T., Barth, M., Knosp, E., Beisteiner, R., 2005. Evaluation of preoperative high magnetic field motor functional MRI (3 Tesla) in glioma patients by navigated electrocortical stimulation and postoperative outcome. J. Neurol. Neurosurg. Psychiatry 76, 1152–1157.

Skare, S., Newbould, R.D., Clayton, D.B., Albers, G.W., Nagle, S., Bammer, R., 2007. Clinical multishot DW-EPI through parallel imaging with considerations of susceptibility, motion, and noise. Magn. Reson. Med. 57, 881–890.

Speck, O., Stadler, J., Zaitsev, M., 2008. High resolution single-shot EPI at 7 T. MAGMA 21, 73–86.

Tallantyre, E.C., Morgan, P.S., Dixon, J.E., Al-Radaideh, A., Brookes, M.J., Evangelou, N., Morris, P.G., 2009. A comparison of 3 T and 7 T in the detection of small parenchymal veins within MS lesions. Invest. Radiol. 44, 491–494.

Triantafyllou, C., Hoge, R.D., Krueger, G., Wiggins, C.J., Potthast, A., Wiggins, G.C., Wald, L.L., 2005. Comparison of physiological noise at 1.5 T, 3 T and 7 T and optimization of fMRI acquisition parameters. Neuroimage 26, 243–250.

van der Zwaag, W., Francis, S., Head, K., Peters, A., Gowland, P., Morris, P., Bowtell, R., 2009. fMRI at 1.5, 3 and 7 T: characterising BOLD signal changes. Neuroimage 47, 1425–1434.

Yacoub, E., Shmuel, A., Pfeuffer, J., Van De Moortele, P.F., Adriany, G., Andersen, P., Vaughan, J.T., Merkle, H., Ugurbil, K., Hu, X., 2001. Imaging brain function in humans at 7 Tesla. Magn. Reson. Med. 45, 588–594.